

## Supplementary Material

### Generalized solid strengthening rule for biocompatible Zn-based alloys, a comparison with Mg-based alloys

Yuanqi Guo<sup>1, 2</sup>, Shihao Zhang<sup>1, 2</sup>, Bo Wei<sup>1, 2</sup>, Dominik Legut<sup>3</sup>, Timothy C. Germann<sup>4</sup>,  
Haijun Zhang<sup>5, 6</sup> and Ruifeng Zhang<sup>1, 2,\*</sup>

<sup>1</sup>*School of Materials Science and Engineering, Beihang University, Beijing 100191, P. R. China*

<sup>2</sup>*Center for Integrated Computational Materials Engineering (International Research Institute for Multidisciplinary Science) and Key Laboratory of High-Temperature Structural Materials & Coatings Technology (Ministry of Industry and Information Technology), Beihang University, Beijing 100191, P. R. China*

<sup>3</sup>*IT4Innovations Center, VSB-Technical University of Ostrava, CZ-70833 Ostrava, Czech Republic.*

<sup>4</sup>*Theoretical Division, Los Alamos National Laboratory, Los Alamos, New Mexico 87545, USA*

<sup>5</sup>*National United Engineering Laboratory for Biomedical Material Modification, Dezhou, Shandong 251100, China*

<sup>6</sup>*Department of Vascular & Intervention, Tenth Peoples' Hospital of Tongji University, Shanghai 200072, China*

\*: Correspondence and requests for materials should be addressed to R.F.Z. (e-mail: zrf@buaa.edu.cn)

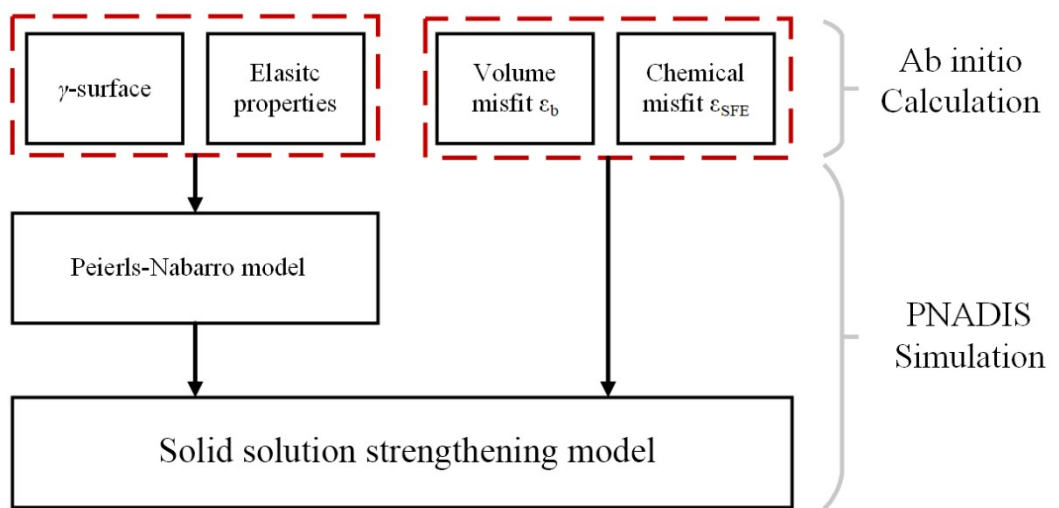


**Figure S1.** The flow chart for the solid solution strengthening calculation. The details of PNADIS code can be referred to our previous publication.<sup>1</sup>

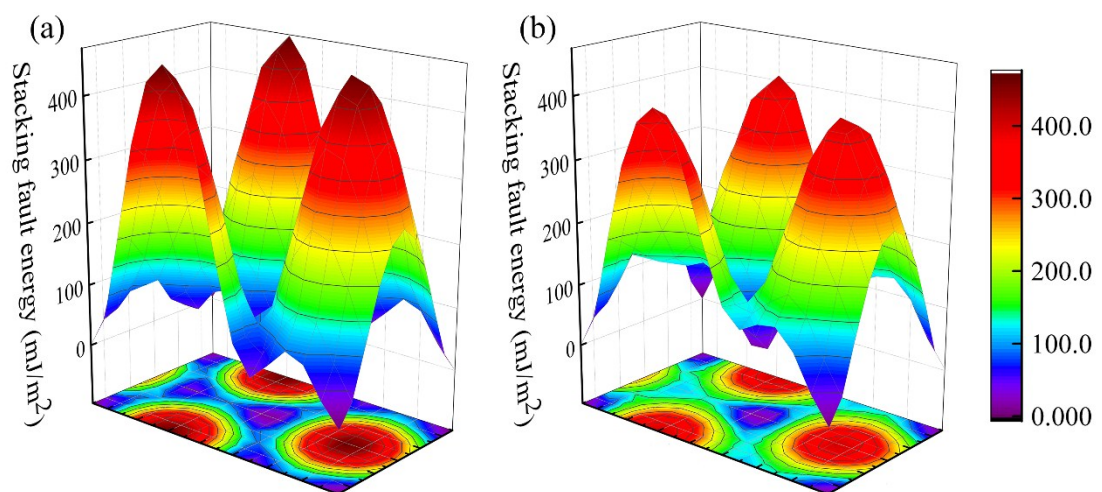


**Figure S2.** The calculated  $\gamma$ -surface for (a) pure Mg and (b) pure Zn.

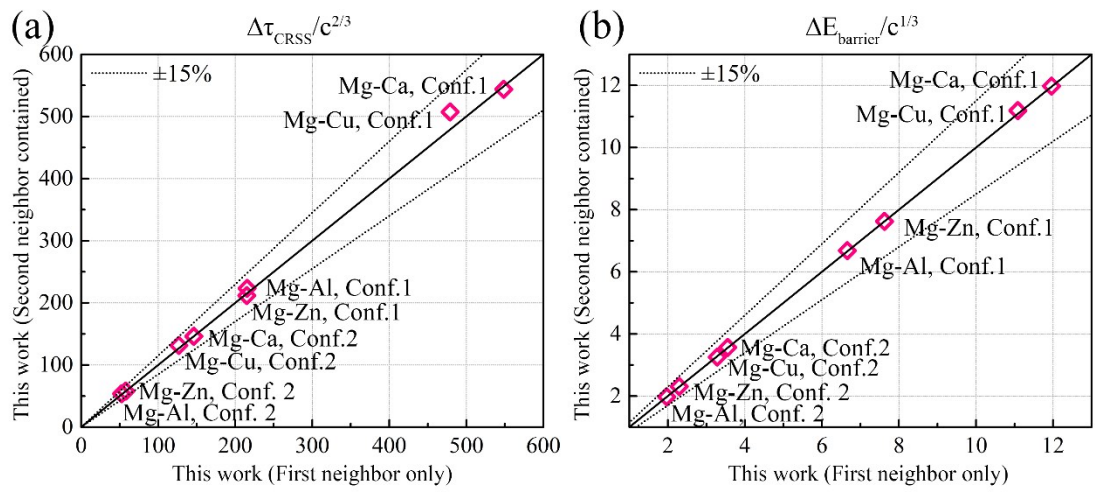


**Figure S3.** The influence of second neighbor SFEs on the predicted (a)  $\Delta\tau_{\text{CRSS}'} / c^{2/3}$  (in MPa) and (b)  $\Delta E_{\text{barrier}'} / c^{1/3}$  (in eV) for several Mg-based alloys.

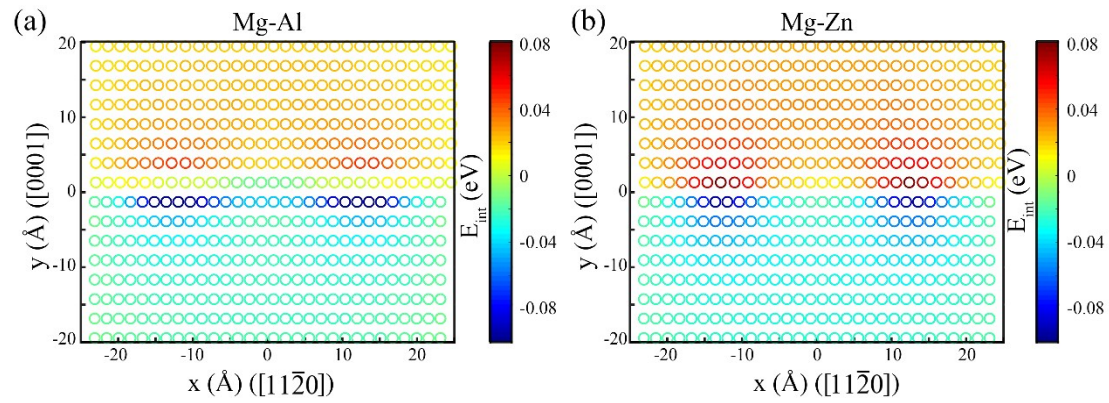


**Figure S4.** The map of solute-dislocation interaction energy with respect to the atomic positions for a basal edge dislocation in (a) Mg-Al and (b) Mg-Zn.

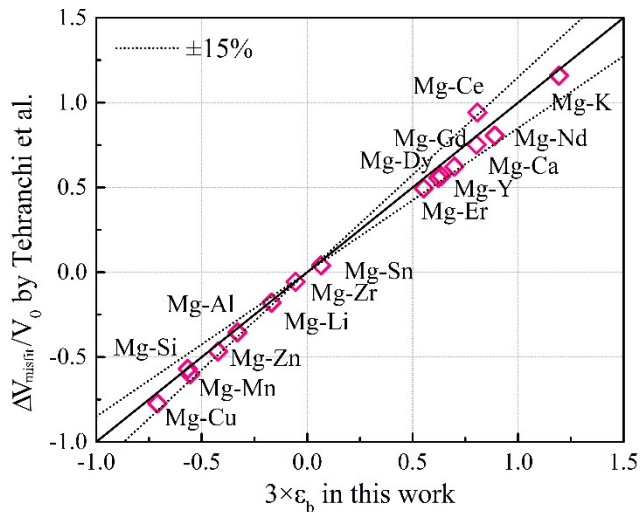


**Figure S5.** A comparison between  $\Delta V_{\text{misfit}}/V_0 = \varepsilon_{11}^m + \varepsilon_{22}^m + \varepsilon_{33}^m$  calculated by Tehranchi et al.<sup>2</sup> and those obtained through  $3 \times \varepsilon_b$ .

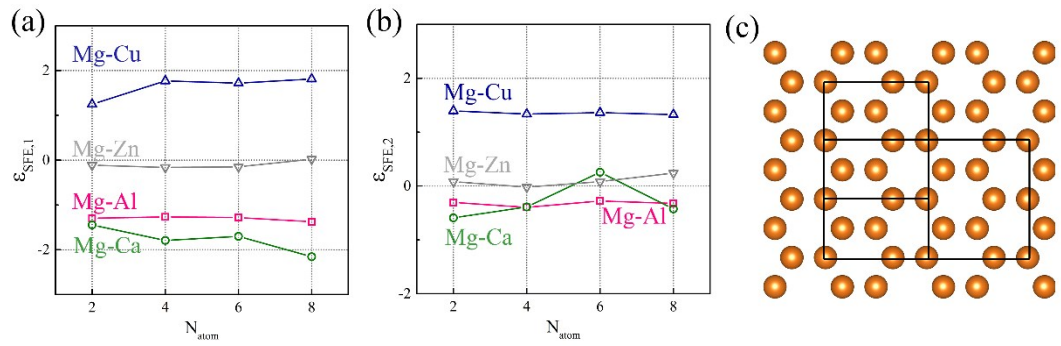


**Figure S6.** The convergence test of (a)  $\varepsilon_{\text{SFE},1}$  and (b)  $\varepsilon_{\text{SFE},2}$  for Mg-Al, Mg-Ca, Mg-Cu and Mg-Zn. (c) The number of atoms per slip plane that corresponds to  $N_{\text{atom}}$  of x-axis in Fig. (a) and (b).

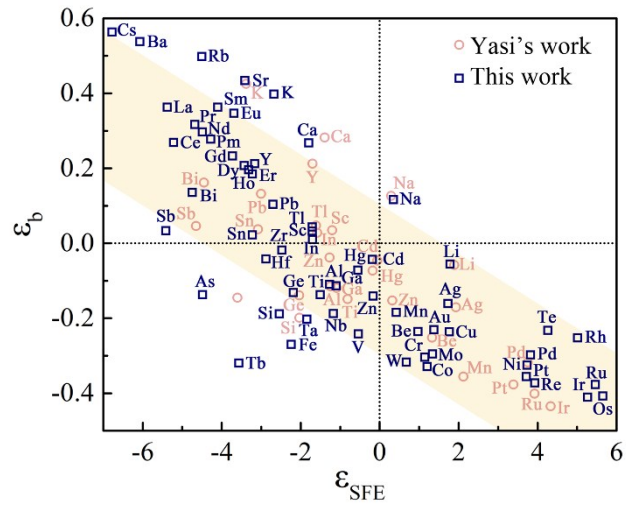


**Figure S7.** Correlation between chemical misfit  $\varepsilon_{SFE}$  on basal (0001) plane and volume misfit  $\varepsilon_b$  in Mg-based alloys. The pink circle symbols indicate the values previously reported for Mg-based alloys by Yasi et al.<sup>3</sup>

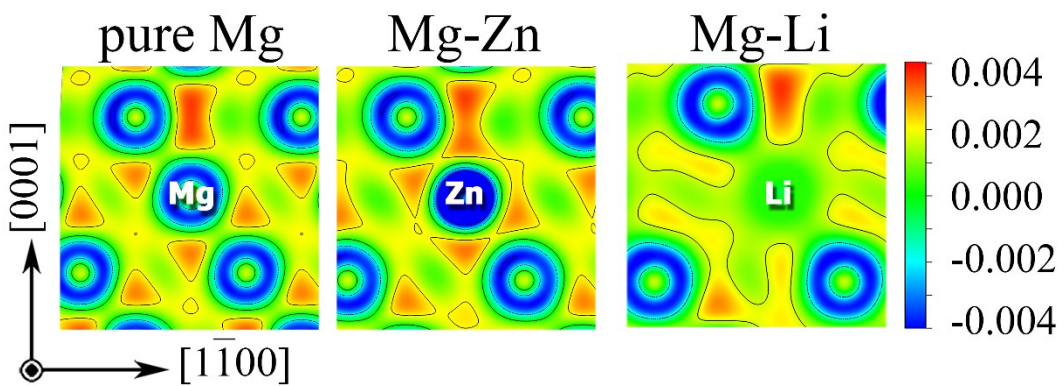


**Figure S8.** The calculated valence charge density differences (VCDD) around  $I_2$ -stacking fault for pure Mg and Mg-based alloys. The unit of VCDD is electrons/Bohr<sup>3</sup>.

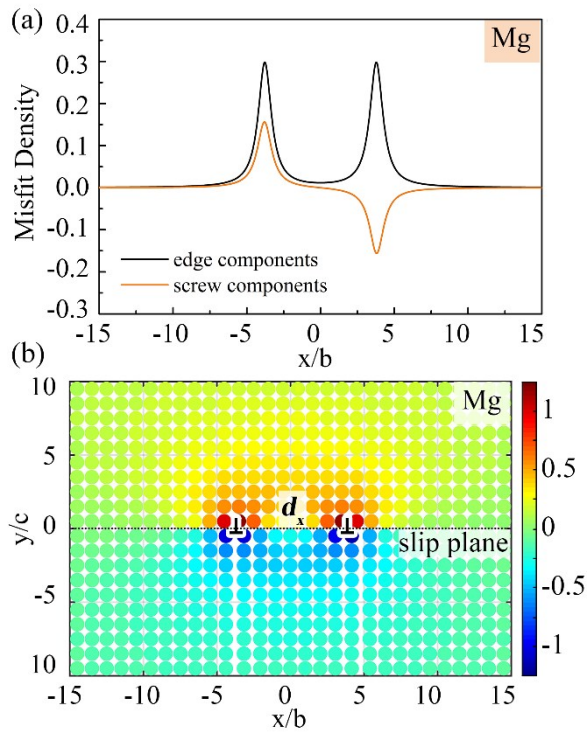


**Figure S9.** (a) The calculated dislocation structure and (b) the pressure field (in GPa) for an edge dislocation of pure Mg, which are obtained by PNADIS code<sup>1</sup>.

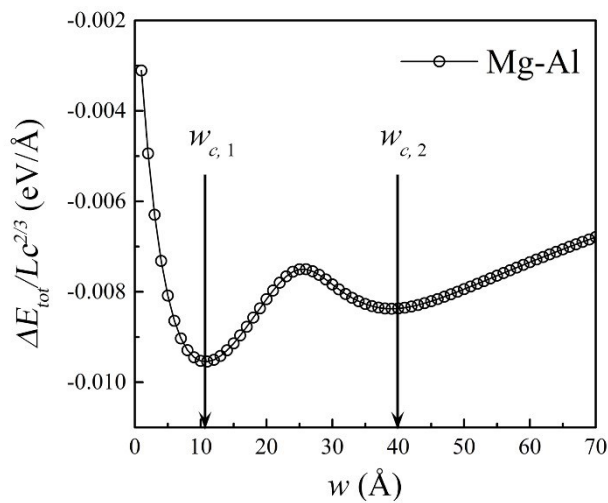


**Figure S10.** The total energy change of a dislocation for Mg-Al alloy during minimization process.

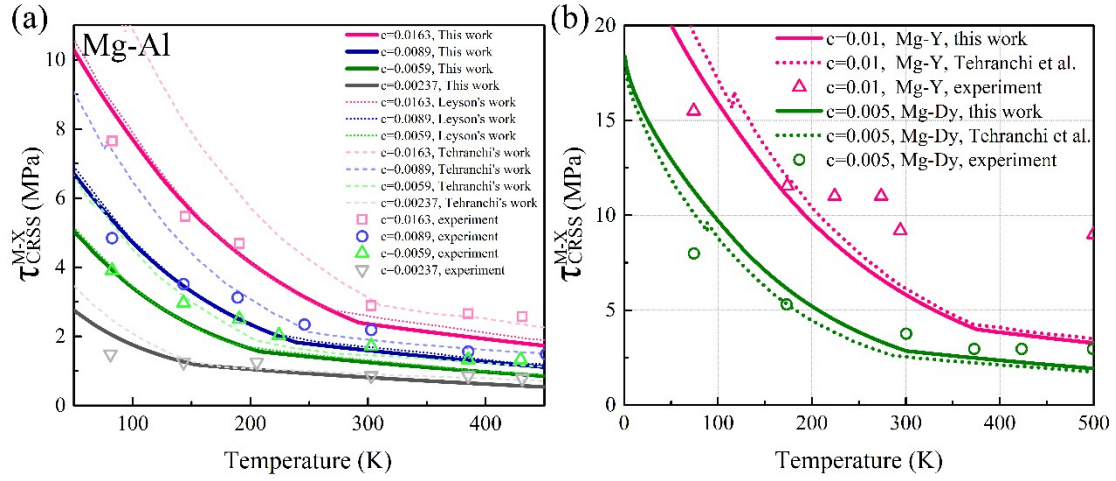


**Figure S11.** (a) The predicted  $\tau_{\text{CRSS}}^{\text{M}-X}$  versus temperature for Mg-Al alloys with different Al-concentration. The solid lines are obtained in the present work, the dot lines indicate other theoretical works<sup>2, 4</sup> and the dot symbols indicate experimental values.<sup>5, 6</sup> (b) The  $\tau_{\text{CRSS}}^{\text{M}-X}$  versus temperature relationships for Mg-Y alloy and Mg-Dy alloy. The results of Tehranchi et al.<sup>2</sup> and experiment values<sup>7</sup> are shown in dot lines and scatters.

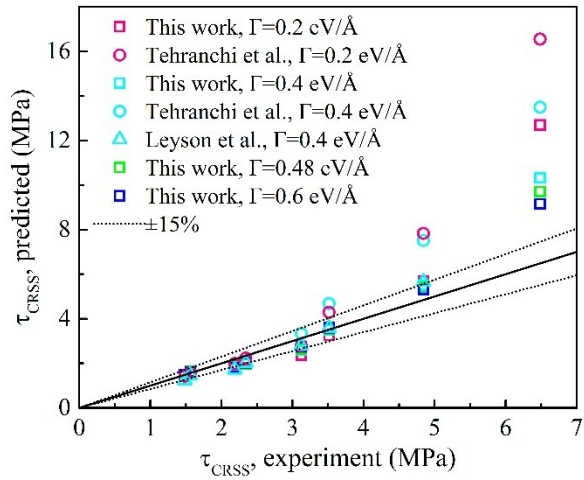


**Figure S12.** The predicted  $\tau_{\text{CRSS}}$  of Mg-0.89%Al alloy under several certain temperatures using different line tension values, compared with the experiment data and previous results by Tehranchi et al.<sup>2</sup> and Leyson et al.<sup>4</sup>

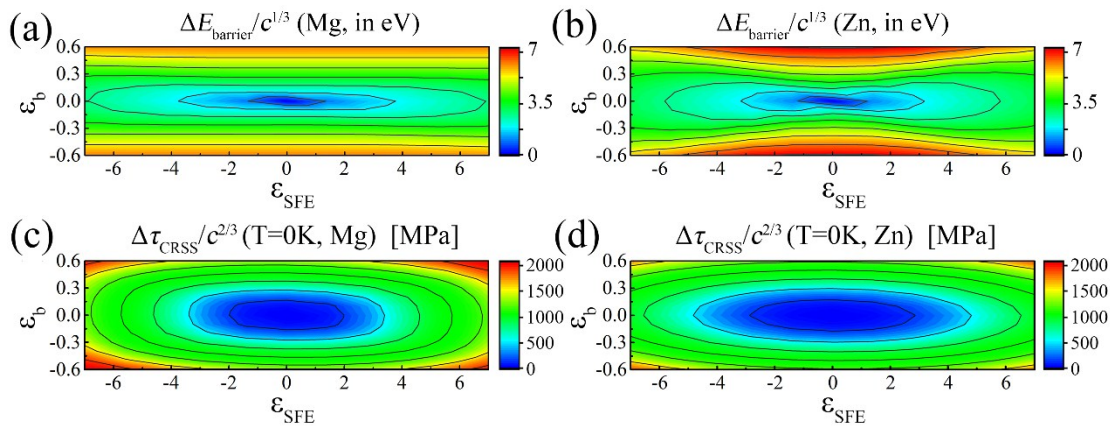


**Figure S13.** The guideline maps of energy barrier  $\Delta E_{\text{barrier}}/c^{1/3}$  for (a) Mg-based alloys and that for (b) Zn-based alloys, and the distribution of  $\Delta \tau_{\text{CRSS}}/c^{2/3}$  for (c) Mg-based and (d) Zn-based alloys.

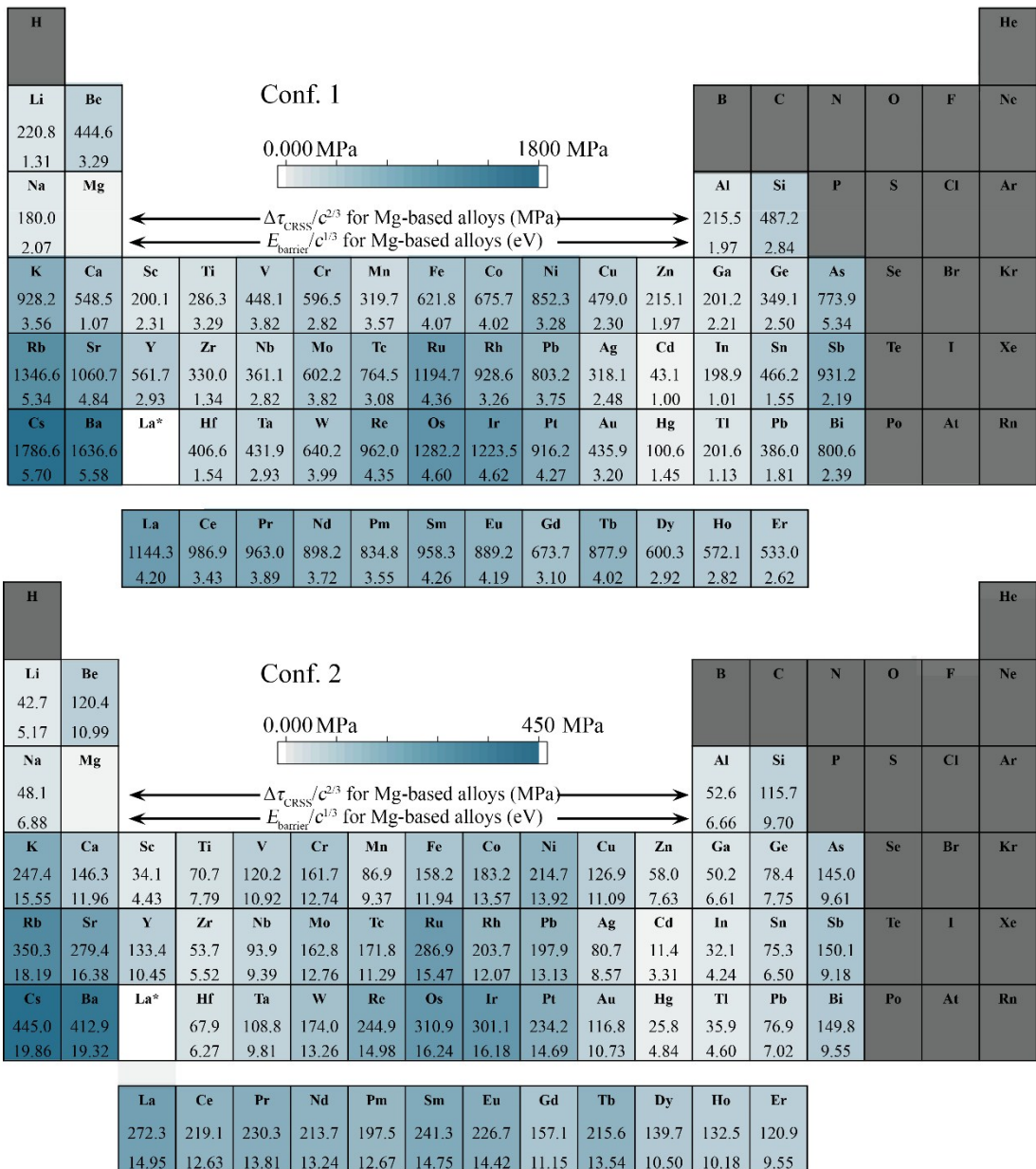


**Figure S14.** The calculated  $\Delta\tau_{\text{CRSS}}/c^{2/3}$  and  $\Delta E_{\text{barrier}}/c^{1/3}$  of an edge dislocation for Mg-based alloys under two configurations, i.e. Conf. 1 and 2. The darker colors mean the better strengthening effect, and lighter colors for the weaker strengthening effect.

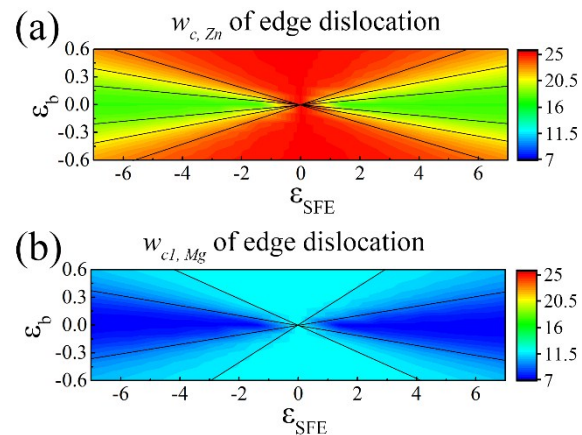


**Figure S15.** Guideline maps for characteristic bow-out distance vs. the misfit parameters  $\varepsilon_b$  and  $\varepsilon_{SFE}$  for (a) Zn and (b) Mg.

**Table S1.** The calculated elastic constants  $C_{ij}$ , the derived Hill average bulk moduli  $B_H$ , shear moduli  $G_H$  and Young's moduli  $E_H$  (all in GPa), and the Poisson ratio  $\nu_H$  of pure Zn and Mg, which are used as the input parameters in the semidiscrete variational P-N model and solid solution strengthening model. Some data from experiments are also listed for comparison.

Material	Source	$C_{11}$	$C_{12}$	$C_{13}$	$C_{33}$	$C_{44}$	$B_H$	$G_H$	$E_H$	$\nu_H$
hcp Zn	This work	164.4	45.2	49.8	53.3	37.5	63.9	37.1	93.2	0.257
	Exp. <sup>8</sup>	160.8	43.1	43.7	54.2	40.0	61.7	39.5	97.7	0.236
	Exp. <sup>9</sup>	163.7	36.4	53.0	63.5	38.8	68.3	39.6	99.6	0.257
	Exp. <sup>10</sup>	179.1	37.5	55.4	68.8	45.95				
	Cal. <sup>11</sup>	156	56	44	68	42				
hcp Mg	This work	68.1	23.7	18.9	70.4	21.0	36.6	22.5	55.9	0.245
	Exp. <sup>12</sup>	59.5	26.12	21.8	61.55	16.35	35.55	17.21	44.45	0.292
	Cal. <sup>13</sup>	69.12	21.84	20.01	70.84	16.37	36.98	20.70	52.34	0.264
	Cal. <sup>14</sup>	63.1	22.2	22.7	66.3	22.6	36.4	21.5	53.8	0.254

**Table S2.** Calculated  $\varepsilon_b$  (volume misfit) and  $\varepsilon_{SFE}$  (chemical misfit) for 61 kinds of Mg-based alloys. The detailed PAW–GGA potential for each element (pv, sv, d, etc.) are marked after element symbol, and \* indicates that the spin-polarization is used.

	$\varepsilon_b$	$\varepsilon_{SFE}$		$\varepsilon_b$	$\varepsilon_{SFE}$
Ag	-0.161	1.735	Nb_pv	-0.188	-1.169
Al	-0.110	-1.267	Nd_3*	0.296	-4.484
As	-0.138	-4.479	Ni*	-0.326	3.735
Au	-0.231	1.377	Os	-0.408	5.654
Ba_sv	0.538	-6.067	Pb_d	0.104	-2.697
Be	-0.236	0.976	Pd*	-0.298	3.825
Bi_d	0.135	-4.739	Pm_3	0.278	-4.275
Ca	0.268	-1.793	Pr_3*	0.317	-4.678
Cd*	-0.043	-0.180	Pt	-0.356	3.717
Ce*	0.269	-5.215	Rb_sv	0.498	-4.499
Co*	-0.329	1.204	Re	-0.373	3.928
Cr	-0.304	1.147	Rh*	-0.253	5.015
Cs_sv	0.563	-6.774	Ru*	-0.377	5.463
Cu	-0.237	1.768	Sb	0.033	-5.413
Dy_3	0.207	-3.425	Sc	0.032	-1.704
Er_3	0.184	-3.220	Si	-0.188	-2.536
Eu_3	0.346	-3.684	Sm_3	0.363	-4.093
Fe*	-0.270	-2.239	Sn_d	0.022	-3.220
Ga_d	-0.114	-1.097	Sr_sv	0.433	-3.411
Gd_3	0.233	-3.723	Ta_pv	-0.203	-1.841
Ge_d	-0.132	-2.183	Tb_3	-0.320	-3.563
Hf_pv	-0.042	-2.875	Tc_pv	-0.233	4.265
Hg	-0.072	-0.545	Ti	-0.138	-1.502
Ho_3	0.195	-3.317	Tl_d	0.043	-1.701
In_d	0.009	-1.700	V	-0.242	-0.536
Ir*	-0.411	5.270	W_pv	-0.317	0.677
K	0.398	-2.675	Y_sv	0.212	-3.159
La*	0.363	-5.374	Zn	-0.141	-0.162
Li_sv	-0.056	1.789	Zr_sv	-0.018	-2.472
Mn*	-0.185	0.427			
Mo_pv	-0.295	1.340			
Na_pv	0.116	0.355			

**Table S3.** Calculated  $\varepsilon_b$  (volume misfit) and  $\varepsilon_{SFE}$  (chemical misfit) for 61 kinds of Zn-based alloys. The detailed PAW–GGA potential for each element (pv, sv, d, etc.) are marked after element symbol, and \* indicates that the spin-polarization is used.

	$\varepsilon_b$	$\varepsilon_{SFE}$		$\varepsilon_b$	$\varepsilon_{SFE}$
Ag	0.117	-0.582	Na_pv	0.250	-1.208
Al	0.055	-1.872	Nb_pv	0.273	-2.226
As	0.219	-4.402	Nd_3*	0.803	-6.942
Au	0.127	-0.806	Ni*	-0.141	-0.654
Ba_sv	1.096	-11.194	Os	0.004	-0.598
Be	-0.167	0.603	Pb_d	0.601	-9.792
Bi_d	0.711	-3.375	Pd*	0.010	-0.844
Ca	0.566	-2.818	Pm_3	0.766	-8.283
Cd*	0.239	-0.438	Pr_3*	0.844	-6.436
Ce*	0.977	-10.113	Pt	0.016	-1.143
Co*	-0.161	-0.896	Rb_sv	0.844	-15.494
Cr	-0.008	-1.537	Re	0.096	-0.361
Cs_sv	1.077	-6.045	Rh*	-0.040	-0.963
Cu	-0.087	0.338	Ru*	-0.012	-0.691
Dy_3	0.638	-5.935	Sb	0.528	-6.786
Er_3	0.597	-5.851	Sc	0.336	-6.224
Eu_3	0.580	-0.264	Si	0.057	-3.993
Fe*	-0.135	-1.933	Sm_3	0.740	-8.411
Ga_d	0.098	-1.950	Sn_d	0.443	-6.960
Gd_3	0.683	-10.819	Sr_sv	0.832	-12.978
Ge_d	0.164	-3.610	Ta_pv	0.274	-2.678
Hf_pv	0.380	-5.977	Tb_3	0.660	-7.888
Hg	0.300	-0.723	Tc_pv	0.072	-0.509
Ho_3	0.618	-6.247	Ti	0.155	-2.871
In_d	0.340	-1.974	Tl_d	0.465	0.241
Ir*	-0.034	-0.877	V	0.058	-2.472
K	0.698	-2.519	W_pv	0.199	-1.402
La*	1.103	-13.737	Y_sv	0.649	-5.880
Li_sv	-0.019	-0.210	Zr_sv	0.414	-7.494
Mg	0.159	-0.427			
Mn*	-0.019	-2.285			
Mo_pv	0.176	-0.877			

**Table S4.** Misfit parameters  $\varepsilon_b$  and  $\varepsilon_{SFE}$  for several alloys compared with other first principle calculations. The calculated energy barrier  $\Delta E_{\text{barrier}}/c^{1/3}$  (in eV) and  $\Delta \tau_{\text{CRSS}}/c^{2/3}$  (in MPa) are listed as well, which are consistent with previous studies.

	$\varepsilon_b$	$\varepsilon_{SFE}$	Conf. 1		Conf. 2		This work
			$\Delta E_{\text{barrier}}/c^{1/3}$	$\Delta \tau_{\text{CRSS}}/c^{2/3}$	$\Delta E_{\text{barrier}}/c^{1/3}$	$\Delta \tau_{\text{CRSS}}/c^{2/3}$	
Mg-Al	-0.110	-1.267	1.97	215.5	6.66	52.6	This work
			1.92	224.4	6.07	63.0	Ref. <sup>4</sup>
			1.94	302.2	6.37	65.8	Ref. <sup>2</sup>
Mg-Y	0.212	-3.159	-0.11	-1.25			Ref. <sup>3</sup>
			2.93	561.7	10.45	133.4	This work
			2.62	575.1	8.47	135.2	Ref. <sup>2</sup>
Mg-Dy	0.21	-3.42	1.5155	381	5.006	89	Ref. <sup>15</sup>
			0.21	-1.70			Ref. <sup>3</sup>
			2.9159	600.3	10.50	139.7	This work
Mg-Zn	-0.14	-0.16	2.65	567.9	8.44	132.9	Ref. <sup>2</sup>
			2.30	215.1	7.63	58.0	This work
			2.23	400.8	7.69	84.6	Ref. <sup>2</sup>
Mg-Gd	-0.153	0.32	-0.153	0.32			Ref. <sup>3</sup>
			3.10	673.7	11.15	157.1	This work
			2.68	656.0	9.06	154.5	Ref. <sup>2</sup>

(Note that the original data in Ref. 2 didn't contain the line tension, and data listed in Table S4 is obtained by the original data in Ref. 2 and our line tension 0.48 eV/Å for Mg-based alloys.)

**Table S5.** Calculated  $w_c$  (in Å),  $\Delta E_{\text{barrier}}/c^{1/3}$  (in eV) and  $\Delta \tau_{\text{CRSS}}/c^{2/3}$  (in MPa) for 61 solutes in Conf. 1 and Conf. 2 of Mg-based alloys.

Conf. 1						Conf. 2						Conf. 1					
	$w_{c1}$	$\Delta E_{\text{barrier}}/c^{1/3}$	$\Delta \tau_{\text{CRSS}}/c^{2/3}$		$w_{c2}$	$\Delta E_{\text{barrier}}/c^{1/3}$	$\Delta \tau_{\text{CRSS}}/c^{2/3}$		$w_{c1}$	$\Delta E_{\text{barrier}}/c^{1/3}$	$\Delta \tau_{\text{CRSS}}/c^{2/3}$		$w_{c2}$	$\Delta E_{\text{barrier}}/c^{1/3}$	$\Delta \tau_{\text{CRSS}}/c^{2/3}$		
Mg-Ag	11.08	2.48	318.1	39.96	8.57	80.7			Mg-Nb	11.56	2.82	361.1	40.36	9.39	93.9		
Mg-Al	10.81	1.97	215.5	38.94	6.66	52.6			Mg-Nd	10.25	3.72	898.2	38.60	13.24	213.7		
Mg-As	8.26	2.50	773.9	35.47	9.61	145.0			Mg-Ni	10.99	4.02	852.3	39.83	13.92	214.7		
Mg-Au	11.80	3.20	435.9	41.03	10.73	116.8			Mg-Os	10.50	4.60	1282.2	39.02	16.24	310.9		
Mg-Ba	11.01	5.58	1636.6	39.86	19.32	412.9			Mg-Pb	8.40	1.81	386.0	35.56	7.02	76.9		
Mg-Be	11.95	3.29	444.6	41.26	10.99	120.4			Mg-Pd	10.71	3.75	803.2	39.38	13.13	197.9		
Mg-Bi	7.94	2.39	800.6	34.95	9.55	149.8			Mg-Pm	10.18	3.55	834.8	38.47	12.67	197.5		
Mg-Ca	11.73	3.56	548.5	40.92	11.96	146.3			Mg-Pr	10.32	3.89	963.0	38.71	13.81	230.3		
Mg-Cd	11.73	1.00	43.1	40.74	3.31	11.4			Mg-Pt	11.18	4.27	916.2	40.11	14.69	234.2		
Mg-Ce	9.42	3.43	986.9	37.10	12.63	219.1			Mg-Rb	11.40	5.34	1346.6	40.44	18.19	350.3		
Mg-Co	11.98	4.07	675.7	41.30	13.57	183.2			Mg-Re	11.12	4.35	962.0	40.03	14.98	244.9		
Mg-Cr	11.97	3.82	596.5	41.28	12.74	161.7			Mg-Rh	9.29	3.26	928.6	36.88	12.07	203.7		
Mg-Cs	10.84	5.70	1786.6	39.60	19.86	445.0			Mg-Ru	10.37	4.36	1194.7	38.81	15.47	286.9		
Mg-Cu	11.64	3.28	479.0	40.79	11.09	126.9			Mg-Sb	7.13	2.19	931.2	34.00	9.18	150.1		
Mg-Dy	9.97	2.92	600.3	38.10	10.50	139.7			Mg-Sc	7.39	1.07	200.1	34.28	4.43	34.1		
Mg-Er	9.67	2.62	533.0	37.54	9.55	120.9			Mg-Si	10.51	2.84	487.2	38.48	9.70	115.7		
Mg-Eu	11.14	4.19	889.2	40.06	14.42	226.7			Mg-Sm	10.99	4.26	958.3	39.82	14.75	241.3		
Mg-Fe	11.29	3.57	621.8	39.81	11.94	158.2			Mg-Sn	7.13	1.55	466.2	34.00	6.50	75.3		
Mg-Ga	11.05	1.97	201.2	39.35	6.61	50.2			Mg-Sr	11.56	4.84	1060.7	40.68	16.38	279.4		
Mg-Gd	10.00	3.10	673.7	38.14	11.15	157.1			Mg-Ta	11.17	2.93	431.9	39.57	9.81	108.8		
Mg-Ge	9.93	2.21	349.1	37.71	7.75	78.4			Mg-Tb	10.88	4.02	877.9	39.05	13.54	215.6		
Mg-Hf	7.42	1.54	406.6	34.35	6.27	67.9			Mg-Tc	9.55	3.08	764.5	37.33	11.29	171.8		
Mg-Hg	11.37	1.45	100.6	39.97	4.84	25.8			Mg-Ti	10.94	2.31	286.3	39.16	7.79	70.7		
Mg-Ho	9.91	2.82	572.1	37.99	10.18	132.5			Mg-Tl	7.63	1.13	201.6	34.56	4.60	35.9		
Mg-In	7.13	1.01	198.9	34.00	4.24	32.1			Mg-V	11.91	3.29	448.1	41.12	10.92	120.2		
Mg-Ir	10.69	4.62	1223.5	39.35	16.18	301.1			Mg-W	12.02	3.99	640.2	41.38	13.26	174.0		
Mg-K	11.72	4.62	928.2	40.91	15.55	247.4			Mg-Y	10.23	2.93	561.7	38.56	10.45	133.4		
Mg-La	10.26	4.20	1144.3	38.60	14.95	272.3			Mg-Zn	11.97	2.30	215.1	41.25	7.63	58.0		
Mg-Li	8.17	1.31	220.8	35.26	5.17	42.7			Mg-Zr	7.25	1.34	330.0	34.14	5.52	53.7		
Mg-Mn	12.02	2.82	319.7	41.37	9.37	86.9											
Mg-Mo	11.93	3.82	602.2	41.22	12.76	162.8											
Mg-Na	11.87	2.07	180.0	41.03	6.88	48.1											

**Table S6.** Calculated  $w_c$  (in Å),  $\Delta E_{\text{barrier}}/c^{1/3}$  (in eV) and  $\Delta \tau_{\text{CRSS}}/c^{2/3}$  (in MPa) for 61 kinds of Zn-based alloys.

	$w_c$	$\Delta E_{\text{barrier}}/c^{1/3}$	$\Delta \tau_{\text{CRSS}}/c^{2/3}$		$w_c$	$\Delta E_{\text{barrier}}/c^{1/3}$	$\Delta \tau_{\text{CRSS}}/c^{2/3}$
Zn-Ag	25.29	6.12	157.2	Zn-Na	25.32	10.15	431.7
Zn-Al	18.91	4.08	167.0	Zn-Nb	24.46	10.62	524.5
Zn-As	20.69	9.07	630.8	Zn-Nd	24.31	21.80	2249.6
Zn-Au	24.98	6.44	181.0	Zn-Ni	25.09	6.90	204.7
Zn-Ba	23.77	26.63	3589.6	Zn-Os	17.70	1.63	32.5
Zn-Be	25.52	7.77	247.0	Zn-Pb	21.68	17.58	2062.9
Zn-Bi	25.33	20.38	1736.0	Zn-Pd	17.85	2.09	52.0
Zn-Ca	25.29	17.50	1286.4	Zn-Pm	23.56	20.93	2277.5
Zn-Cd	25.69	9.90	392.5	Zn-Pr	24.62	22.63	2330.8
Zn-Ce	23.72	24.65	3094.3	Zn-Pt	17.93	2.58	78.5
Zn-Co	24.86	7.52	250.5	Zn-Rb	21.10	22.13	3543.0
Zn-Cr	17.66	3.05	114.9	Zn-Re	25.50	5.37	118.3
Zn-Cs	25.15	26.81	3068.9	Zn-Rh	19.78	3.02	80.3
Zn-Cu	25.48	5.03	103.8	Zn-Ru	18.11	1.92	42.0
Zn-Dy	24.09	18.65	1691.5	Zn-Sb	22.82	16.20	1501.6
Zn-Er	23.91	17.79	1573.7	Zn-Sc	21.06	11.98	1044.6
Zn-Eu	25.72	17.87	1275.0	Zn-Si	17.95	5.96	416.9
Zn-Fe	21.95	6.50	272.0	Zn-Sm	23.36	20.41	2220.8
Zn-Ga	20.72	5.29	213.7	Zn-Sn	21.86	14.36	1340.8
Zn-Gd	21.82	19.16	2400.9	Zn-Sr	21.89	21.85	3091.6
Zn-Ge	20.31	7.57	464.7	Zn-Ta	23.92	10.60	557.1
Zn-Hf	21.85	12.96	1093.1	Zn-Tb	23.14	18.86	1950.3
Zn-Hg	25.65	11.51	533.4	Zn-Tc	24.77	4.38	85.7
Zn-Ho	23.80	18.18	1665.8	Zn-Ti	21.05	7.15	372.1
Zn-In	25.11	12.42	662.3	Zn-Tl	25.69	15.41	951.8
Zn-Ir	19.56	2.76	69.1	Zn-V	18.50	4.65	232.0
Zn-K	25.52	20.17	1663.7	Zn-W	24.79	8.65	333.8
Zn-La	22.96	26.52	3945.9	Zn-Y	24.17	18.88	1716.7
Zn-Li	23.13	1.80	17.7	Zn-Zr	21.17	13.76	1356.3
Zn-Mg	25.63	7.54	229.7				
Zn-Mn	17.74	4.02	197.0				
Zn-Mo	25.29	8.03	271.1				

## Reference

1. S. H. Zhang, D. Legut and R. F. Zhang, *Comput. Phys. Commun.*, 2019, **240**, 60-73.
2. A. Tehranchi, B. Yin and W. A. Curtin, *Acta Mater.*, 2018, **151**, 56-66.
3. J. A. Yasi, L. G. Hector and D. R. Trinkle, *Acta Mater.*, 2010, **58**, 5704-5713.
4. G. P. M. Leyson, L. G. Hector and W. A. Curtin, *Acta Mater.*, 2012, **60**, 5197-5203.
5. A. Akhtar and E. Teghtsoonian, *Acta Metall.*, 1969, **17**, 1339-1349.
6. A. Akhtar and E. Teghtsoonian, *Philos. Mag.*, 1972, **25**, 897-916.
7. S. Miura, S. Imagawa, T. Toyoda, K. Ohkubo and T. Mohri, *Mater. Trans.*, 2008, 0804070382-0804070382.
8. E. Griineisen and E. Goens, *Z. Fur Physik.*, 1924, **26**, 235.
9. G. A. Alers and J. R. Neighbours, *J. Phys. Chem. Solids*, 1958, **7**, 58-64.
10. G. Simmons and H. Wang, *Single crystal elastic constants and calculated aggregate properties*, The M.I.T. Press, Cambridge, 1971.
11. M. De Jong, I. Winter, D. C. Chrzan and M. Asta, *Physical Review B*, 2017, **96**, 014105.
12. A. R. Wazzan and L. B. Robinson, *Phys. Rev.*, 1967, **155**, 586.
13. S. H. Zhang, I. J. Beyerlein, D. Legut, Z. H. Fu, Z. Zhang, S. L. Shang, Z. K. Liu, T. C. Germann and R. F. Zhang, *Phys. Rev. B*, 2017, **95**, 224106.
14. C. Wang, H. Y. Wang, T. L. Huang, X. N. Xue, F. Qiu and Q. C. Jiang, *Sci Rep*, 2015, **5**, 10213.
15. D. Buey, L. Hector Jr and M. Ghazisaeidi, *Acta Mater.*, 2018, **147**, 1-9.